Journal of Neuroimaging in Psychiatry & Neurology

http://dx.doi.org/10.17756/jnpn.2016-004

Research Article

Open Access

Associations between ^{18}F-AV133 Cerebral VMAT2 Binding and Plasma LDL and HDL Levels in Parkinson's Disease

Rui Gao[1,2*], Guangjian Zhang[3], Xueqi Chen[2,4], Savina Reid[2] and Yun Zhou[2*]

[1]*Department of Nuclear Medicine, the First Affiliated Hospital of Xian Jiaotong University, Xi'an, Shaanxi, China*
[2]*The Russell H. Morgan Department of Radiology and Radiological Science, Johns Hopkins University School of Medicine, Baltimore, MD, USA*
[3]*Department of Surgery, the First Affiliated Hospital of Xian Jiaotong University, Xi'an, Shaanxi, China*
[4]*Department of Nuclear Medicine, Peking University First Hospital, Beijing, China*

[*]**Correspondence to:**
Yun Zhou
The Russell H. Morgan Department of Radiology and Radiological Science
Johns Hopkins University School of Medicine
601 N. Caroline Street, JHOC room 3241
Baltimore, MD 21287-0807, USA
Fax: +1 410 955 0696
E-mail: yunzhou@jhmi.edu

Rui Gao
Department of Nuclear Medicine
The First Affiliated Hospital of Xian Jiaotong University, Xi'an, Shaanxi, 710061, China
Fax: +86 029 85323644
E-mail: jacky_mg@163.com

Received: October 29, 2015
Accepted: March 11, 2016
Published: March 14, 2016

Citation: Gao R, Zhang G, Chen X, Reid S, Zhou Y. 2016. Associations between ^{18}F-AV133 Cerebral VMAT2 Binding and Plasma LDL and HDL Levels in Parkinson's Disease. *J Neuroimaging Psychiatry Neurol* 1(1): 20-26.

Published by United Scientific Group

Abstract

Purpose: The primary objective of this study was to investigate associations between cerebral presynaptic vesicular monoamine transporter 2 (VMAT2) density and plasma lipid levels in Parkinson's disease (PD) using quantitative ^{18}F-9-fluoropropyl-(+)-dihydrotetrabenazine (^{18}F-AV133) positron emission tomography (PET).

Methods: Ten-min ^{18}F-AV133 PET scans, acquired 80 min post tracer injection, and structural MRI scans for 22 PD patients and four healthy controls were collected from the Parkinson's Progression Markers Initiative study (PPMI) project. Serum lipid measurements were available for six of the 22 patients. The ^{18}F-AV133 cerebral standardized uptake value ratio (SUVR) relative to the occipital cortex was calculated as an index of VMAT2 density. SPSS and statistical parametric mapping (SPM) software were used to analyze the relationships between lipid indicators (including total cholesterol, high-density lipoprotein (HDL), low density lipoprotein (LDL), and triglycerides), and SUVRs in both regions of interest (ROI) and voxelwise levels.

Results: ROI based analysis revealed significant positive linear correlations between serum LDL levels and SUVRs of the medial temporal lobe, amygdala, left anterior putamen, substantia nigra, midbrain and serum LDL levels (r: 0.91 to 0.99, $p < 0.01$, n = 6). Negative correlations were found between serum HDL and the SUVRs of the caudate, left posterior putamen, and ventral striatum (r: -0.98 to -0.93, $p < 0.01$, n = 6). SPM analysis showed there were positive correlations between LDL and SUVRs in the right amygdala and uncus. Prominent negative correlations between HDL levels and SUVRs were found in the left caudate and ventral striatum.

Conclusion: This pilot study provided evidence of a strong linear correlation between cerebral VMAT2, measured by ^{18}F-AV133 PET, and plasma LDL, HDL levels in PD patients. This correlation indicates that cholesterol might play an important role in the Parkinson's disease progression.

Keywords

PET, ^{18}F-AV133, Parkinson's disease, VMAT2, LDL, HDL

Introduction

Vesicular monoamine transporter 2 (VMAT2) is the protein responsible for transporting both dopamine and serotonin into synaptic vesicles [1]. ^{11}C-dihydrotetrabenazine (^{11}C-DTBZ) PET has been used for *in vivo* imaging of

cerebral VMAT2, and has proved to be a potential quantitative biomarker for monitoring dopaminergic degeneration in Parkinson's disease (PD) [2-4]. One major limitation of the tracer preventing its wide use is its short physical half-life (20 min). ^{18}F-9-fluoropropyl-(+)-dihydrotetrabenazine (^{18}F-DTBZ, or ^{18}F-AV133 hereafter) is a recently developed PET tracer with a 110 min physical half-life for clinical quantitative VMAT2 imaging [5]. Previous studies show that ^{18}F-AV133 is a promising PET tracer for detecting and monitoring the VMAT2 reduction in PD patients [6-11].

Dysregulation of lipid metabolism in the brain appears to be linked to chronic neurodegenerative disorders, including Alzheimer's disease and PD [12-16]. Although the findings are still controversial, the overall evidence favors an association between higher total cholesterol and lower PD risk [13, 17]. Recent reports revealed a direct relationship between higher cholesterol levels and a slowing in the rate of decline in Parkinson's disease patients [18].

Since cholesterol metabolism is associated with Parkinson's disease pathogenesis and progression [13, 18], and VMAT2 imaging has proven to be an objective marker for monoaminergic neuron synaptic integrity [6, 9, 19], it is plausible to predict a similar correlation between the monoamine neuronal integrity marker and serum lipid levels. To evaluate this hypothesis, we investigated the associations between plasma lipid indicators (including total cholesterol, high-density lipoprotein (HDL), low density lipoprotein (LDL), and triglycerides) and cerebral VMAT2 densities assessed by ^{18}F-AV133 PET in PD patients.

Materials and Methods

The available online data from the Parkinson's Progression Markers initiative (PPMI) database (http://www.ppmi-info.org/data) were downloaded in December 2014, which include patient demographics, clinical assessment, plasma lipids indicators, ^{18}F-AV133 PET, and MRI images. As described below in more detail, the downloaded ^{18}F-AV133 PET images were then processed and analyzed at both regions of interest and voxelwise levels. The relationships between HDL, LDL, and ^{18}F-AV133 SUVRs in both region of interest (ROI) and voxelwise levels were analyzed.

^{18}F-AV133 PET and MRI acquisition and image processing

^{18}F-AV133 PET scans (http://www.ppmi-info.org/: AV-133 PET Imaging Technical Operations Manual, Version 1.2 Final, July 2012) and T1 weighted structural MRI scans using magnetization prepared rapid acquisition gradient echo sequence, or fast spoiled gradient-recalled-echo sequence, (http://www.ppmi-info.org/: MRI Technical Operations Manual, Version 4, 2012) were collected from the PPMI project by December 2014 for 22 patients with Parkinson's disease and four controls. The PET and MRI scans at the screening or first visit were included in the study. All subjects were drug naïve for Parkinson's disease medication. 10 min (2 × 5 min) ^{18}F-AV133 images acquired at 80.8 (± 2.8 SD) min post tracer injection was used in the study.

All PET and MRI images were processed using Statistical Parametric Mapping software (Wellcome Department of Imaging Neuroscience, London, United Kingdom) SPM8 (http://www.fil.ion.ucl.ac.uk/spm/software/spm8/) and MATLAB (The MathWorks Inc.). To study the spatial and temporal changes of ^{18}F-AV133 VMAT2 binding in PD progression, the PET and MRI images of the PD patients were reoriented so that the striatum contralateral to the symptomatic side was always on the left of the brain [20]. To minimize motion effects during PET scans, the ^{18}F-AV133 images with two frames were first aligned to generate mean images. The aligned 10 min ^{18}F-AV133 PET mean images were then coregistered to MRI images. The MRI images were normalized to standard Montreal Neurologic Institute (MNI) space using SPM8 [21] with a high resolution MRI template provided by VBM8 toolbox [22]. The transformation parameters determined by MRI spatial normalization were then applied to the coregistered PET images for PET spatial normalization. A total of 34 regions of interest (ROIs), including the cortex, striatum, and sub-striatum regions, were manually drawn on the MRI template using PMOD software (PMOD Technologies Ltd., Zürich, Switzerland) in standard MNI space. The sub-striatum regions used in the study were the ventral striatum, caudate, anterior putamen (pre-commissural dorsal putamen), and posterior putamen (post-commissural putamen) [23, 24]. The occipital cortex was used as reference tissue to calculate the standardized uptake value ratio (SUVR) of ^{18}F-AV133 binding (http://www.ppmi-info.org/: AV-133 PET Image Processing Methods for Calculation of Striatal Binding Ratio), where the SUVR is a quantitative measurement of VMAT2 density in brain tissues. SUVR images were calculated as PET (images)/PET (occipital) in the standard space (image volume: 121 × 145 × 121, voxel size: 1.5 × 1.5 × 15 mm in x, y, z). ROI SUVRs were then obtained by applying ROIs to SUVR images. A 3D spatial Gaussian filter of 8 mm full width at half maximum in x, y, z direction was applied to SUVR images for voxelwise statistical analysis using SPM8.

Plasma lipid indicator evaluation

Among the 22 PD patients with ^{18}F-AV133 PET images, serum lipid measurements were available for six of them. All subjects were comprehensively assessed at the screening and baseline visits for clinical characteristics (motor, neuropsychological, and cognitive) and plasma indicators as described in the PPMI biologics manual (http://www.ppmi-info.org/). Details of this study have previously been reported [25], and up-to-date information on the study can be obtained from the project webpage.

Statistical analysis

Analyses were performed with Statistical Package for the Social Sciences (SPSS) statistics (version 21; SPSS, Inc., Chicago, IL, USA). PD patients were sub-grouped into severely disabled (SD - PD, Motor Scale > 32) and mild-to-moderately disabled (MD - PD, Motor Scale ≤ 32) based on their evaluations with the unified Parkinson disease rating scale (UPDRS) Part III (Motor scale) [26]. Comparisons of baseline serum lipids concentrations, ROI SUVRs between Parkinson's disease, sub-groups, and controls were tested with independent t-tests. The Mann-Whitney's U test was used in

case of non-normally distributed variables, and the chi-square test was used for categorical data. The relationships between the baseline plasma indicators and ROI SUVRs were explored by Pearson's correlations and $p < 0.01$ was set as a significant level. Voxelwise statistical analysis was performed using SPM8 in the study. Statistical parametric maps were obtained for each serum lipid indicator by linear regression between SUVR images and serum lipid concentrations. For the relatively higher noise levels of voxelwise SUVR measurements, results of linear regressions were reported at a p-value < 0.001 for clusters > 50 voxels.

Results

Demographics and clinical assessments

Demographic statistics and clinical assessments for the participants with [18]F-AV133 PET scans are listed in Table 1. The UPDRS motor scales in the PD group were significantly higher than those in controls, while the Montreal Cognitive Assessment (MoCA) between PD patients and controls (HCs) were not significantly different.

Table 1: Demographics and clinical assessments of subjects with [18]F-AV133 PET.

	PD patients		HCs (n=4)	*P**
	All (n=22)	With lipid levels (n=6)		
Age (years)	64.51 (33.7-77.3)	66.83 (61.5-69.4)	63.37 (57.7-66.7)	0.71
Gender (male: female)	18:4	5:1	3:1	0.44
Disease duration (months)	18.19 (2-23)	12.00 (5-18)	/	/
UPDRS Part III (Motor Scale)	22.64 (8-45)	24.67 (15-35)	0	0.00
Hoehn and Yahr stage	1.60 (0-2)	1.67 (1-2)	/	/
MoCA	25.50 (17-30)	25.0 (22-28)	27.75 (27-29)	0.05
Side predominantly affected at onset (R: L)	14:8	4:2	/	/

HC, Healthy controls; PD, Parkinson's disease; UPDRS, unified Parkinson disease rating scale; MoCA, Montreal cognitive assessment. Data are presented as mean (range). *Comparison between 22 PDs and 4 HCs.

[18]F-AV133 cerebral VMAT2 binding in HCs and Parkinson's disease

The simple statistics of ROI SUVRs of the [18]F-AV133 binding in HCs and PD group are illustrated in Figure 1. The SUVRs in the Parkinson's disease group (n = 22) were remarkably reduced in striatal sub-regions in the following order: left posterior putamen, right posterior putamen (54.1%, 43.2%) > left anterior putamen, right anterior putamen (35.6%, 27.9%) > left caudate, right caudate (24.5%, 20.8%) as compared to healthy controls (n = 4). The SUVRs of the cerebellum, ventral striatum, substantia nigra, and midbrain in the Parkinson's disease group were reduced by 5-12% from healthy controls, but not statistically significant ($p > 0.2$). The SUVRs in the medial temporal, amygdala, and hippocampus were almost equivalent between the Parkinson's disease group and healthy controls ($p > 0.64$). As expected, when comparing the cerebral VMAT2 densities between PD and healthy controls, the SPM analysis revealed two prominent clusters (> 5000 voxels). In PD patients, the clusters located in the bilateral caudate and putamen with higher T values in left side showed unsymmetrical decrease in striatal VMAT2 density (Figure 2).

Further analysis showed that there was no significant difference in SUVRs between the MD - PD group (n = 17) and the SD - PD group (n = 5) ($p > 0.10$); however, there was a trend of reduced

SUVR in the left posterior putamen, left caudate, left ventral striatum, substantia nigra, and midbrain (p: 0.10-0.40). Correspondingly, the cognitive measurements of the MoCA score in the SD - PD group were slightly lower than those in the MD - PD group (25.20 ± 2.14 *vs.* 26.12 ± 3.18, $p = 0.57$).

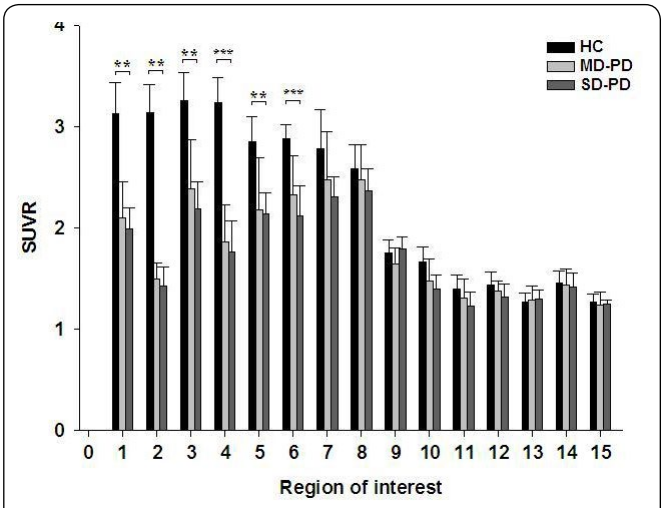

Figure 1: The mean ± standard deviation of ROI SUVRs of [18]F-AV133 in healthy controls (HC) (n = 4), mild disabled PD patients (n = 17), and severely disabled PD patients (n = 5). Regions of interest are numbered as: 1: left anterior putamen; 2: left posterior putamen; 3: right anterior putamen; 4: right posterior putamen; 5: left caudate; 6: right caudate; 7: left ventral striatum; 8: right ventral striatum; 9: dorsal raphe nucleus; 10: substantia nigra; 11: midbrain; 12: cerebellum; 13: medial temporal cortex; 14: amygdala; 15: hippocampus. The SUVR in striatum subregions in PD group (n = 22) were significant lower than ones in healthy controls (n = 4) (***: $p < 0.001$, **: $p = 0.01$).

Correlation between plasma lipid levels and [18]F-AV133 VMAT2 binding in PD patients

The correlation analysis was based on the six PD patients who had both [18]F-AV133 PET imaging and serum lipid assessments. The mean [18]F-AV133 SUVR images of the six PD patients are shown in Figure 3. There were no significant differences in all ROI SUVRs between the six patients and all 22 PD patients ($p > 0.15$).

We first used an ROI approach for our analysis. There were significant positive linear correlations between the SUVRs of

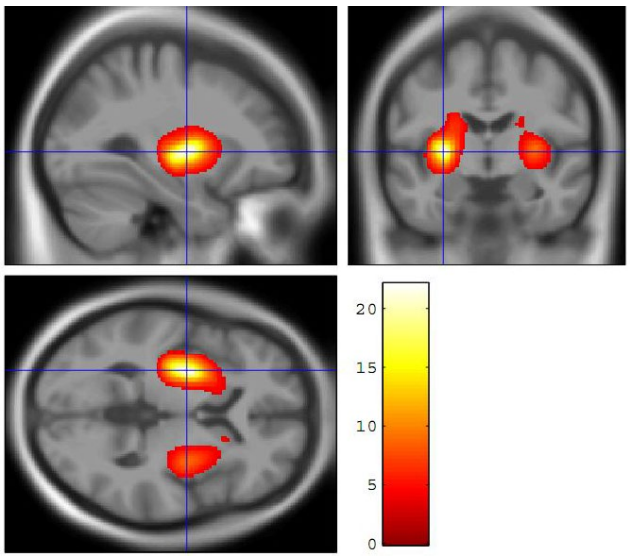

Figure 2: Differences of cerebral VMAT2 density between healthy controls and Parkinson's disease patients from voxelwsie statistical analysis using SPM8. Results showed unsymmetrical decrease in striatal VMAT2 density in PD as compared with healthy controls, which is consistent with the results obtained in region of interest based analysis (Figure 1).

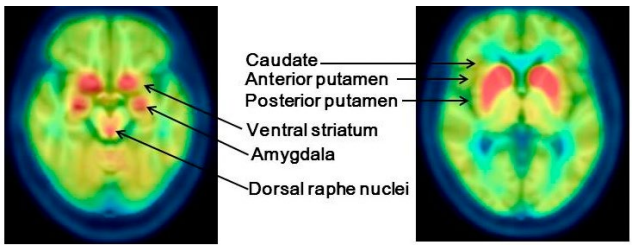

Figure 3: The mean [18]F-AV133 SUVR images of the 6 PD patients (4 mild disabled PD and 2 severely disabled PD patients) with plasma lipid levels. The ROI [18]F-AV133 SUVRs (mean ± SD) in left posterior putamen, right posterior putamen, left anterior putamen, right anterior putamen, caudate, ventral striatum, amygdala, dorsal raphe nuclei were 1.48 ± 0.37, 1.61 ± 0.67, 2.03 ± 0.71, 2.13 ± 0.10, 2.05 ± 0.70, 2.30 ± 0.92, 1.36 ± 0.50, 1.54 ± 0.63 in the 6 PD patients

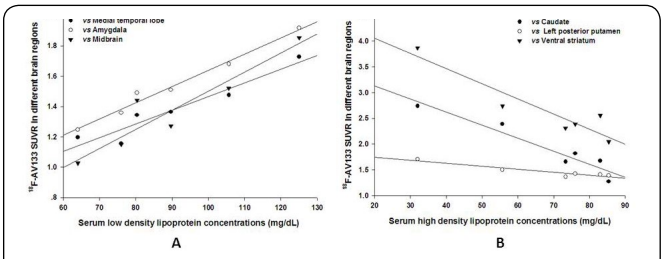

Figure 4: Linear correlation between plasma lipoprotein levels and [18]F-AV133 VMAT2 binding in PD patients (n = 6). A: ROI based analysis showed a significant positive correlation between LDL levels and [18]F-AV133 SUVRs in the medial temporal lobe (Y = 0.009X + 0.563, R^2 = 0.916), amygdala (Y = 0.011X + 0.571, R^2 = 0.981), and midbrain (Y = 0.0126X + 0.244, R^2 = 0.881). B: HDL levels were negatively correlated with SUVRs in the caudate (Y = -0.0253X + 3.636, R^2 = 0.916), left posterior putamen (Y = -0.0058X + 1.86, R^2 = 0.88) and ventral striatum (Y = -0.0294X + 4.639, R^2 = 0.871).

the medial temporal lobe, amygdala, left anterior putamen, substantia nigra, midbrain and serum LDL levels (Pearson r: 0.91 to 0.99, p < 0.01, n = 6). The typical linear correlation

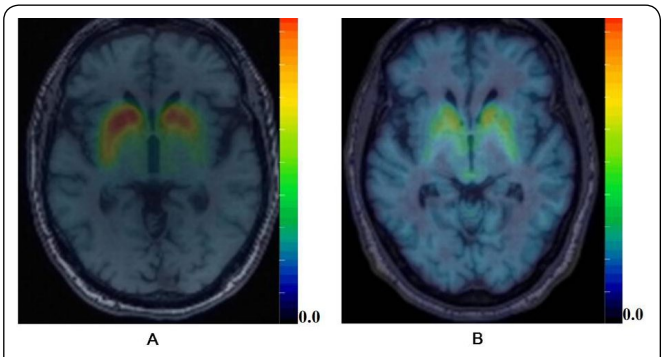

Figure 5: Representative [18]F-AV133 SUVR images of PD patients with different LDL and HDL levels. **A:** a 69.8-y-old male with HDL/LDL of 32.0/125.0 mg/dL; **B:** a 53.9-y-old male with HDL/LDL levels of 73.3/64.0 mg/dL. The UPDRS motor scale/MoCA score for the patient **A** and **B** were 17/27 and 35/24, respectively. [18]F-AV133 ROI SUVRs of patient A and B were: caudate, 2.74 and 2.29; left putamen, 2.47 and 1.87; right putamen, 3.47 and 2.19; ventral striatum, 3.87 and 2.72; raphe nuclei, 2.09 and 1.60; and substantia nigra, 2.12 and 1.51, respectively.

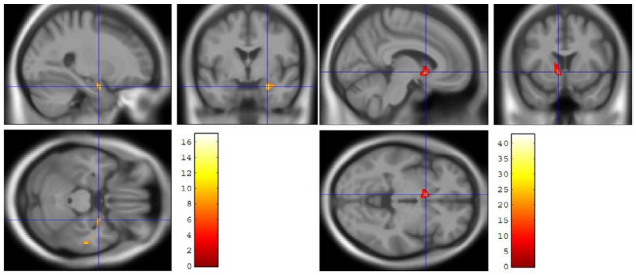

Figure 6: Statistical t map on MRI template. **A**: voxel SUVRs in the cluster (right amygdala and uncus) were correlated with serum LDL levels; and **B**: voxel SUVR in the cluster (left caudate and ventral striatum) were correlated with serum HDL levels. p < 0.001 and cluster > 50 voxels were selected in SPM analysis.

between amygdala SUVR and LDL levels is illustrated in Figure 4A. In contrast, there were negative linear correlations between [18]F-AV133 SUVRs of the caudate, left posterior putamen, and ventral striatum, hippocampus and HDL levels in PD patients with Pearson r: -0.98 to -0.81 (p < 0.01). The typical linear correlation between caudate SUVR and HDL levels is demonstrated in Figure 4B. A representative SUVR image from a typical PD patient with low HDL/high LDL (patient A) showed a higher SUVR and better UPDRS motor scale/MoCA score as compared to patient B with high HDL/low LDL (Figure 5).

SPM analysis was also performed in our study. The SPM map of serum LDL level correlations revealed a cluster (91 voxels; peak T = 13.89 at 26 mm, -3 mm, -24 mm in x, y, z) that mainly covered right amygdala and uncus (Figure 6A). With regards to serum HDL levels correlations, the most prominent negative correlations between HDL levels and SUVRs were found in the left caudate and ventral striatum (252 voxels; peak T = 42.76 at -8 mm, 11 mm, -5 mm in x, y, z) (Figure 6B), and another small cluster (81 voxels) was mainly located in the parahippocampal gyrus.

Discussion

The main finding of this study showed a linear correlation between cerebral VMAT2 densities measured by [18]F-AV133

specific binding and plasma LDL and HDL levels in PD patients. This study also confirmed that VMAT2 densities are significantly lower in the striatal sub regions in PDs as compared with controls.

[18]F-9-fluoropropyl-(+)-dihydrotetrabenazine ([18]F-AV-133) is a novel positron emission tomography (PET) tracer for imaging VMAT2 in monoaminergic neurons [6, 19, 27]. Successful imaging studies have demonstrated the feasibility of [18]F-AV-133 to differentiate normal controls from PD subjects [6, 27]. A recent publication clearly indicated the sensitivity of [18]F-AV-133 for detecting monoaminergic terminal reductions in PD patients and concluded that [18]F-AV-133 may allow the selection of presymptomatic patients with nigrostriatal movement disorders [6]. Consistent with previous reports, the current [18]F-AV-133 PET study showed significantly lower VMAT2 densities in PD patients in the following order: posterior putamen>anterior putamen>caudate [6]. The SPM analysis confirmed that the posterior putamen was the most severely affected striatal subregion, followed by the anterior putamen and caudate nucleus [20].

Since VMAT2 is a transporter not only for dopamine, but also for serotonin, norepinephrine, histamine, and GABA [28-32], the reductions in VMAT2 PET measurements reflect the brain dysfunction in PD related to those mentioned neurons. It is demonstrated that the decrease of VMAT2 level was correlated with the non-motor symptoms [33]. Our results showed that [18]F-AV133 PET imaging could detect the monoaminergic degeneration in these extrastriatal regions. The SUVRs of the amygdala, cerebellum, substantia nigra, midbrain and medial temporal lobe were 5-12% lower than healthy controls (to 67.7-92.5% SUVR of putamen, Figure 1). These reductions are believed to be manifestations of small vessel cerebrovascular diseases [34] that may contribute to decreased blood flow and [18]F-AV133 binding.

The current PET study showed high correlations between the [18]F-AV133 SUVRs of the medial temporal lobe, amygdala, substantia nigra, midbrain and serum LDL levels, whilst the [18]F-AV133 SUVRs of striatum subregions revealed significant negative correlations with HDL levels in Parkinson's disease (Figures 4 and 6). Thus, our findings provide evidence for a close relationship between VMAT2 density and serum lipoprotein levels in patients with PD [35]. This strong correlation suggests that the lipoproteins played a crucial role in the monoaminergic neuron synaptic functions [36-39]. Based on the present results, high serum lipid levels may have a beneficial effect on improving the monoaminergic neuron integrity and thus slowing PD progression. In addition, the present findings suggest that lowering plasma cholesterol with statins should be considered cautiously in PD patients, as has been indicated by Huang et al. [17]. Their study showed that statin usage was associated with higher risk of PD after accounting for serum LDL-cholesterol levels, which is inconsistent with the hypothesis that statins might be neuroprotective for PD [40].

It has long been acknowledged that the decrease of serum lipids is associated with the impairment in cognitive functioning [41, 42]. In support of that, our whole brain ROI analysis and SPM tests showed close correlations between LDL and monoaminergic neuronsin brain areas associated with cognitive functioning (mainly limbic lobe, temporal lobe, and amygdala). This LDL-related hypo-excitation of cortical and sub-cortical areas as a result of degeneration of monoaminergic neurons may underlie the cognitive deficits in PD patients [43]. In order to investigate whether plasma lipids play a role in the cognitive deficit in PD, we analyzed plasma lipid concentrations in PDs with serum lipid and lipoprotein concentrations in PPMI. Results showed that the levels of LDL in cognitively normal PD patients (MoCA total score ≥ 26) were significantly higher than in cognitively declined PD patients (p = 0.01, data not shown).

The significant negative correlation found between [18]F-AV133 VMAT2 binding in striatal subregions with HDL leads to the proposition that HDL levels may indicate motor dysfunction in Parkinson's disease. Although we did not find correlations between UPDRS motor scores and HDL levels, HDL concentrations in mild-moderate disabled patients differed from severely disabled Parkinson's disease in the hypothesized direction (HDL in mild-moderate disabled PD patients (58.7 ± 37.7, n = 2) < ones in severely disabled PD patients (72.0 ± 11.6, n = 4)). As the relatively small sample size may make it difficult to reach statistical significance, further large sample, longitudinal follow-up studies are needed.

Conclusions

In conclusion, this pilot study provided evidence of a strong linear correlation between cerebral VMAT2 densities measured by [18]F-AV133 specific binding and plasma LDL and HDL levels in PD patients, indicating that cholesterol defects might play an important role in the Parkinson's disease progression. Though a higher significance level (p > 0.001) and cluster size were adopted in the SPM analysis to make the analysis more reliable, the small sample size was still a limitation of this research. A large number of PD patients for further validation are needed.

Acknowledgements

Data used in the preparation of this article were obtained from the PPMI database (www.ppmi-info.org/data). For up-to-date information on the study, visit www.ppmi-info.org. PPMI-a public-private partnership-is funded by the Michael J. Fox Foundation for Parkinson's Research and funding partners, including AbbVie, Avid Radiopharmaceuticals, Biogen Idec, Bristol-Myers Squibb, Covance, GE Healthcare, Genentech, GlaxoSmithKline, Lilly, Lundbeck, Merck, Meso Scale Discovery, Pfizer Inc., Piramal Imaging, Roche, Servier, and UCB.

References

1. Guillot TS, Miller GW. 2009. Protective actions of the vesicular monoamine transporter 2 (VMAT2) in monoaminergic neurons. *Mol Neurobiol* 39(2): 149-170. doi: 10.1007/s12035-009-8059-y
2. Bohnen NI, Albin RL, Koeppe RA, Wernette KA, Kilbourn MR, et al. 2006. Positron emission tomography of monoaminergic vesicular binding in aging and Parkinson disease. *J Cereb Blood Flow Metab* 26(9):

1198-1212. doi: 10.1038/sj.jcbfm.9600276

3. Koeppe RA, Frey KA, Kume A, Albin R, Kilbourn MR, et al. 1997. Equilibrium versus compartmental analysis for assessment of the vesicular monoamine transporter using (+)-alpha-[11C] dihydrotetrabenazine (DTBZ) and positron emission tomography. *J Cereb Blood Flow Metab* 17(9): 919-931. doi: 10.1097/00004647-199709000-00001
4. Koeppe RA, Frey KA, Kuhl DE, Kilbourn MR. 1999. Assessment of extrastriatal vesicular monoamine transporter binding site density using stereoisomers of [11C]dihydrotetrabenazine. *J Cereb Blood Flow Metab* 19(12): 1376-1384. doi: 10.1097/00004647-199912000-00011
5. Lin KJ, Weng YH, Wey SP, Hsiao I, Lu CS, et al. 2010. Whole-body biodistribution and radiation dosimetry of 18F-FP-(+)-DTBZ (18F-AV-133): a novel vesicular monoamine transporter 2 imaging agent. *J Nucl Med* 51(9): 1480-1485. doi: 10.2967/jnumed.110.078196
6. Hsiao IT, Weng YH, Lin WY, Hsieh CJ, Wey SP, et al. 2014. Comparison of 99mTc-TRODAT-1 SPECT and 18F-AV-133 PET imaging in healthy controls and Parkinson's disease patients. *Nucl Med Biol* 41(4): 322-329. doi: 10.1016/j.nucmedbio.2013.12.017
7. Kung MP, Hou C, Goswami R, Ponde DE, Kilbourn MR, et al. 2007. Characterization of optically resolved 9-fluoropropyl-dihydrotetrabenazine as a potential PET imaging agent targeting vesicular monoamine transporters. *Nucl Med Biol* 34(3): 239-246. doi: 10.1016/j.nucmedbio.2006.12.005
8. Lin KJ, Weng YH, Hsieh CJ, Lin WY, Wey SP, et al. 2013. Brain imaging of vesicular monoamine transporter type 2 in healthy aging subjects by 18F-FP-(+)-DTBZ PET. *PLoS One* 8(9): e75952. doi: 10.1371/journal.pone.0075952
9. Siderowf A, Pontecorvo MJ, Shill HA, Mintun MA, Arora A, et al. 2014. PET imaging of amyloid with Florbetapir F18 and PET imaging of dopamine degeneration with 18F-AV-133 (florbenazine) in patients with Alzheimer's disease and Lewy body disorders. *BMC Neurol* 14: 79. doi: 10.1186/1471-2377-14-79
10. Toomey JS, Bhatia S, Moon LT, Orchard EA, Tainter KH, et al. 2012. PET imaging a MPTP-induced mouse model of Parkinson's disease using the fluoropropyl-dihydrotetrabenazine analog [18F]-DTBZ (AV-133). *PLoS One* 7(6): e39041. doi: 10.1371/journal.pone.0039041
11. Wood H. 2014. Parkinson disease: 18F-DTBZ PET tracks dopaminergic degeneration in patients with Parkinson disease. *Nat Rev Neurol* 10(6): 305. doi: 10.1038/nrneurol.2014.81
12. de Lau LM, Bornebroek M, Witteman JC, Hofman A, Koudstaal PJ, et al. 2005. Dietary fatty acids and the risk of Parkinson disease: the Rotterdam study. *Neurology* 64(12): 2040-2045. doi: 10.1212/01.WNL.0000166038.67153.9F
13. de Lau LM, Koudstaal PJ, Hofman A, Breteler MM. 2006. Serum cholesterol levels and the risk of Parkinson's disease. *Am J Epidemiol* 164(10): 998-1002. doi: 10.1093/aje/kwj283
14. Huang X, Chen H, Miller WC, Mailman RB, Woodard JL, et al. 2007. Lower low-density lipoprotein cholesterol levels are associated with Parkinson's disease. *Mov Disord* 22(3): 377-381. doi: 10.1002/mds.21290
15. Simon KC, Chen H, Schwarzschild M, Ascherio A. 2007. Hypertension, hypercholesterolemia, diabetes, and risk of Parkinson disease. *Neurology* 69(17): 1688-1695. doi: 10.1212/01.wnl.0000271883.45010.8a
16. Mahlknecht P, Sprenger F, Seppi K, Poewe W. 2015. Plasma fasting cholesterol profiles and age at onset in Parkinson's disease. *Mov Disord* 30(14): 1974-1975. doi: 10.1002/mds.26452
17. Huang X, Alonso A, Guo X, Umbach DM, Lichtenstein ML, et al. 2015. Statins, plasma cholesterol, and risk of Parkinson's disease: A prospective study. *Mov Disord* 30(4): 552-559. doi: 10.1002/mds.26152.
18. Huang X, Auinger P, Eberly S, Oakes D, Schwarzschild M, et al. 2011. Serum cholesterol and the progression of Parkinson's disease: results from DATATOP. *PLoS One* 6(8): e22854. doi: 10.1371/journal.pone.0022854
19. Chao KT, Tsao HH, Weng YH, Hsiao IT, Hsieh CJ, et al. 2012. Quantitative analysis of binding sites for 9-fluoropropyl-(+)-dihydrotetrabenazine ([18F] AV-133) in a MPTP-lesioned PD mouse model. *Synapse* 66(9): 823-831. doi: 10.1002/syn.21572
20. Wang J, Zuo CT, Jiang YP, Guan YH, Chen ZP, et al. 2007. 18F-FP-CIT PET imaging and SPM analysis of dopamine transporters in Parkinson's disease in various Hoehn & Yahr stages. *J Neurol* 254(2): 185-190.
21. Ashburner J, Friston KJ. 2005. Unified segmentation. *Neuroimage* 26(3): 839-851. doi: 10.1016/j.neuroimage.2005.02.018
22. Gaser C. 2014. Voxel-based morphometry extension to SPM8.
23. Martinez D, Slifstein M, Broft A, Mawlawi O, Hwang DR, et al. 2003. Imaging human mesolimbic dopamine transmission with positron emission tomography. Part II: amphetamine-induced dopamine release in the functional subdivisions of the striatum. *J Cereb Blood Flow Metab* 23(3): 285-300. doi: 10.1097/01.WCB.0000048520.34839.1A
24. Mawlawi O, Martinez D, Slifstein M, Broft A, Chatterjee R, et al. 2001. Imaging human mesolimbic dopamine transmission with positron emission tomography: I. Accuracy and precision of D(2) receptor parameter measurements in ventral striatum. *J Cereb Blood Flow Metab* 21(9): 1034-1057. doi: 10.1097/00004647-200109000-00002
25. Kang JH, Irwin DJ, Chen-Plotkin AS, Siderowf A, Caspell C, et al. 2013. Association of cerebrospinal fluid β-amyloid 1-42, T-tau, P-tau181, and α-synuclein levels with clinical features of drug-naive patients with early Parkinson disease. *JAMA Neurol* 70(10): 1277-1287. doi:10.1001/jamaneurol.2013.3861
26. Martínez-Martín P, Rodríguez-Blázquez C, Mario Alvarez, Arakaki T, Arillo VC, et al. 2015. Parkinson's disease severity levels and MDS-Unified Parkinson's disease rating scale. *Parkinsonism Relat Disord* 21(1): 50-54. doi: 10.1016/j.parkreldis.2014
27. Okamura N, Villemagne VL, Drago J, Pejoska S, Dhamija RK, et al. 2010. *In vivo* measurement of vesicular monoamine transporter type 2 density in Parkinson disease with (18) F-AV-133. *J Nucl Med* 51(2): 223-228. doi: 10.2967/jnumed.109.070094
28. Eiden LE, Schäfer MK, Weihe E, Schütz B. 2004. The vesicular amine transporter family (SLC18): amine/proton antiporters required for vesicular accumulation and regulated exocytotic secretion of monoamines and acetylcholine. *Pflugers Arch* 447(5): 636-640. doi: 10.1007/s00424-003-1100-5
29. Eiden LE, Weihe E. 2011. VMAT2: a dynamic regulator of brain monoaminergic neuronal function interacting with drugs of abuse. *Ann N Y Acad Sci* 1216: 86-98. doi: 10.1111/j.1749-6632.2010.05906.x
30. Schafer MK, Weihe E, Eiden LE. 2013. Localization and expression of VMAT2 aross mammalian species: a translational guide for its visualization and targeting in health and disease. *Adv Pharmacol* 68: 319-334. doi: 10.1016/B978-0-12-411512-5.00015-4
31. Stoessl AJ. 2014. Developments in neuroimaging: positron emission tomography. *Parkinsonism Relat Disord* 20(Suppl 1): S180-S183. doi: 10.1016/S1353-8020(13)70042-7
32. Tritsch NX, Ding JB, Sabatini BL. 2012. Dopaminergic neurons inhibit striatal output through non-canonical release of GABA. Nature 490(7419): 262-266. doi: 10.1038/nature11466
33. Brooks DJ, Piccini P. 2006. Imaging in Parkinson's disease: the role of monoamines in behavior. *Biol Psychiat* 59(10): 908-918. doi: 10.1016/j.biopsych.2005.12.017
34. Ichikawa H, Mukai M, Ohno H, Shimizu Y, Itaya K, et al. 2012. Deep white matter hyperintensities, decreased serum low-density lipoprotein, and dilative large arteriopathy. *J Stroke Cerebrovasc Dis* 21(3): 225-230. doi: 10.1016/j.jstrokecerebrovasdis.2010.07.002
35. Lee CS, Samii A, Sossi V, Ruth TJ, Schulzer M, et al. 2000. *In vivo* positron emission tomographic evidence for compensatory changes in presynaptic dopaminergic nerve terminals in Parkinson's disease. *Ann Neurol* 47(4): 493-503. doi: 10.1002/1531-8249(200004)47:4<493::AID-ANA13>3.0.CO;2-4

36. Linetti A, Fratangeli A, Taverna E, Valnegri P, Francolini M, et al. 2010. Cholesterol reduction impairs exocytosis of synaptic vesicles. *J Cell Sci* 123(4): 595-605. doi: 10.1242/jcs.060681

37. Pfrieger FW. 2003. Role of cholesterol in synapse formation and function. *Biochim Biophys Acta* 1610(2): 271-280. doi: 10.1016/S0005-2736(03)00024-5

38. Thiele C, Hannah MJ, Fahrenholz F, Huttner WB. 2000. Cholesterol binds to synaptophysin and is required for biogenesis of synaptic vesicles. *Nat Cell Biol* 2(1): 42-49. doi: 10.1038/71366

39. Segatto M, Leboffe L, Trapani L, Pallottini V. 2014. Cholesterol homeostasis failure in the brain: implications for synaptic dysfunction and cognitive decline. *Curr Med Chem* 21(24): 2788-2802. doi: 10.2174/092986732166140303142902

40. Tan EK, Tan LC. 2013. Holding on to statins in Parkinson disease. *Neurology* 81(5): 406-407. doi: 10.1212/WNL.0b013e31829d87bb

41. Tsui-Pierchala BA, Encinas M, Milbrandt J, Johnson EM Jr. 2002. Lipid rafts in neuronal signaling and function. *Trends Neurosci* 25(8): 412-417. doi: 10.1016/S0166-2236(02)02215-4

42. Solomon A, Kåreholt I, Ngandu T, Winblad B, Nissinen A, et al. 2007. Serum cholesterol changes after midlife and late-life cognition: twenty-one-year follow-up study. *Neurology* 68(10): 751-756. doi: 10.1212/01.wnl.0000256368. 57375. b7

43. Van Vliet P. 2012. Cholesterol and late-life cognitive decline. *J Alzheimers Dis* 30: S147-S162. doi: 10.3233/JAD-2011-111028